Reduction of spin transfer by synthetic antiferromagnets

N. C. Emley,[a] F. J. Albert, E. M. Ryan, I. N. Krivorotov, D. C. Ralph, and R. A. Buhrman
Cornell University, Ithaca, New York 14853-2501

J. M. Daughton and A. Jander
NVE Corporation, Eden Prairie, Minnesota 55344

(Received 27 January 2004; accepted 2 April 2004; published online 7 May 2004)

Synthetic antiferromagnetic layers (SAF) are incorporated into spin transfer nanopillars giving a layer composition $[Co_{bottom}/Ru/Co_{fixed}]/Cu/Co_{free}$, where square brackets indicate the SAF. The Co_{bottom} and Co_{fixed} layers are aligned antiparallel (AP) by strong indirect exchange coupling through the Ru spacer. All three magnetic layers are patterned, so this AP alignment reduces undesirable dipole fields on the Co_{free} layer. Adding the Co_{bottom}/Ru layers reduces the spin polarization of the electron current passing through the nanopillar, leading to a decreased spin-torque per unit current incident on the Co_{free} layer. This may be advantageous for device applications requiring a reduction of the effects of a spin-torque, such as nanoscale current-perpendicular-to-plane magnetoresistive read heads. © *2004 American Institute of Physics.* [DOI: 10.1063/1.1757638]

The reversal of a thin ferromagnetic layer by application of a spin-polarized current, or spin transfer effect (ST), has been extensively studied in systems with the familiar $Co_{fixed}/Cu/Co_{free}$ current-perpendicular-to-plane (CPP) pseudo-spin valve composition[1–4] as well as other magnetic trilayers.[5,6] The prevailing theories[7,8] indicate that the spin-polarized current applies a spin-torque, local to the Cu/Co_{free} interface, that can induce a dynamical response from the Co_{free} magnetization. Such dynamics, although important for the study of ST, are parasitic for more passive devices such as CPP giant magnetoresistance (GMR) read heads, where the Co_{free} layer is sensitive to stray fields from magnetic bits on a hard drive medium.[9] ST-induced dynamics would give erroneous signals in nanoscale devices and so it is advantageous to minimize the effects of a spin-torque in such devices.

In this letter we present the results of an experiment where a third, oppositely aligned magnetic layer (Co_{bottom}) has been incorporated into the CPP spin valve structure adjacent to the Co_{fixed} layer. We investigate field H and a dc current I-induced switching of the Co_{free} layer in structures with layer composition $Cu(100)/Co_{bottom}(11.5)/Ru(0.7)/Co_{fixed}(8)/Cu(6)/Co_{free}(2)/Cu(2)/Pt(30)$ (in nm), where all three Co layers are patterned in a nanopillar geometry. Interlayer exchange coupling through the thin Ru spacer gives a strong antiparallel (AP) alignment of the two adjacent Co layers.[10] The $Co_{bottom}/Ru/Co_{fixed}$ trilayer thus forms a synthetic antiferromagnet (SAF), where magnetostatic fields from the two Co layers are in opposition and the overall dipolar coupling to the Co_{free} layer is reduced.

All layers are dc sputter-deposited in a 1 mTorr Ar ambient onto thermally oxidized Si wafer substrates. Base pressures are $\leqslant 3\times10^{-8}$ Torr. Electron beam lithography, reactive ion etching, and evaporation are used to define a mask which protects the underlying layers during an ion beam etch step. The etching is timed to stop partway through the thick Cu buffer, patterning all three Co layers. SiO_2 is deposited with a plasma enhanced chemical vapor deposition process. Photolithography, subsequent ion beam etching steps, and sputter deposition define top and bottom leads in a four-point CPP configuration. Resistance measurements are made at $T=295$ K using a Wheatstone bridge and lock-in amplifier technique with a 25 μA excitation current i_{ex}. Here, negative I indicates electron flow from the SAF to the Co_{free} layer.

Figure 1(a) shows the device GMR ($I=0$) with H ap-

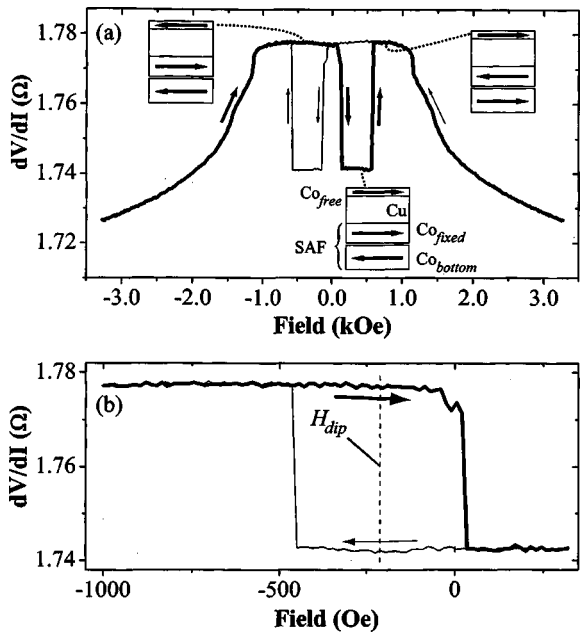

FIG. 1. (a) High-field GMR of the SAF nanopillar. Simulated devices are shown to indicate the alignment of the three magnetizations as the field is swept from negative to positive values. Resistance jumps at $H\approx150$ and 600 Oe are reversals of the Co_{free} layer and SAF pair, respectively. (b) Low-field GMR of the same device. The field is scanned asymmetrically to isolate the switching of the Co_{free} layer. The dipolar field ($H_{dip}^{SAF}\approx-220$ Oe) is taken as the offset of the hysteresis loop, indicated by the dashed line.

[a]Electronic mail: nce2@cornell.edu

plied in-plane. The continuing decrease in dV/dI at the maximum H is the gradual breaking of the SAF AP alignment.[11] To distinguish between switching events for $|H|<1.0$ kOe, we use a Stoner–Wolfarth simulation where total energy (Zeeman, anisotropy, interlayer exchange, and dipole field) is minimized for all three layers at each 4 Oe increment in H. This simulation confirms the different magnetic configurations, shown pictorially in Fig. 1(a). For $H\approx150$ Oe the switch from high to an intermediate resistance state corresponds to the reversal of the Co_{free} layer. A smaller coercivity is expected for the Co_{free} layer due to its smaller shape anisotropy H_{an}^{shape} (~thickness). The jump back to high resistance at $H\approx600$ Oe is the reversal of the Co_{bottom} layer, which in turn switches the Co_{fixed} layer via the strong interlayer coupling. We do not observe any temporary deviation from AP alignment within the SAF that may occur during this jump in resistance.

In Fig. 1(b) the magnetic field is scanned over an asymmetric range, -1000 Oe$<H<300$ Oe, in order to isolate the switching of the Co_{free} layer. The offset of this hysteresis loop is taken as the dipole field on the Co_{free} layer $|H_{dip}^{SAF}|\approx220$ Oe. The two thicknesses of the SAF magnetic layers are chosen specifically to minimize the combined dipole field halfway through the Co_{free} layer. Imperfections in the magnetic layers during fabrication are most likely responsible for $H_{dip}^{SAF}\neq0$. Dipole field calculations from surface currents on an isolated magnetic disk (i.e., no SAF pair) show $|H_{dip}|\approx400$ Oe halfway through the Co_{free} layer. The resistance changes in Fig. 1(b) shift in H as a bias I is applied (shown in Fig. 3), a further indication that the minor loop is the Co_{free} layer switching since the SAF is too thick to be affected by the spin-torque.[12]

Looking at the resistance area product (ΔRA) from the GMR of 35 SAF samples, we find $(\Delta RA)_{SAF}=0.45\pm0.07$ m$\Omega\,\mu$m^2. For 59 normal samples without the Co_{bottom}/Ru layers but with identical thicknesses for the rest of the trilayer, we measure $(\Delta RA)_{normal}=0.94\pm0.19$ m$\Omega\,\mu$m^2, almost a factor of 2 larger. This reduction of ΔRA for the SAF samples is attributed to the reduced polarization of the electrons that pass through and are reflected from the SAF trilayer compared to the case of a single Co fixed layer. Both the Co_{bottom} and the Co_{fixed} layers in the SAF are considerably thinner than the room temperature spin-diffusion length of Co ($\ell_{sf}^{Co}\approx38$ nm[13]), and the Ru coupling layer is also much thinner (0.7 nm) than its spin-diffusion length (~14 nm[14]). Consequently, all of the interfaces of the SAF play a role in the spin-filtering[15] and collectively determine the net spin polarization of the current that impinges onto the Co_{free} layer in these near-ballistic ST devices.

While the spin-filtering that results from the electronic structure of the two Co/Ru interfaces[16,17] and any bulk spin-dependent scattering that does occur can be expected to modify the effect, the two oppositely aligned magnetizations of the SAF pair will clearly reduce the spin current amplitude that passes through or, depending on the bias current direction, reflects off the SAF. Since the magnetoresistance signal ΔRA is, in the ballistic limit, linearly dependent upon the effective polarization η_{eff} of this current, the reduced magnetoresistance signal from SAF devices indicates that

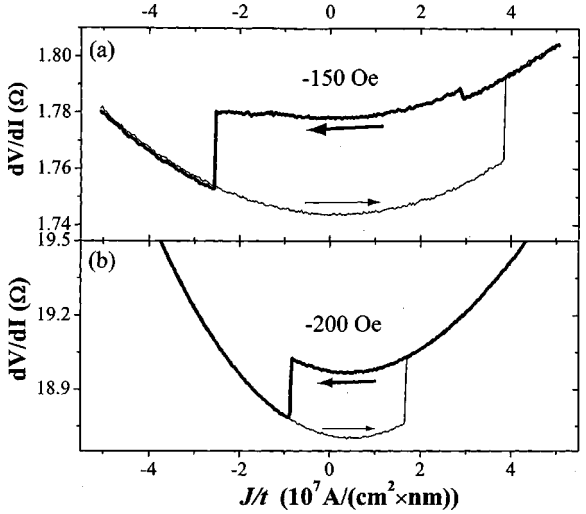

FIG. 2. dV/dI vs current density normalized to the free layer thickness J/t for (a) a 90×190 nm elliptical SAF sample and (b) a 70×130 nm elliptical normal sample. The resistance values in (b), a two-point measurement, include lead resistance ~6 Ω and contact resistance ~9 Ω.

$\eta_{eff}\approx\frac{1}{2}\eta_{Co}$ where η_{Co} is the polarization produced by the spin filtering of a single fixed Co layer.

We note that the ΔRA for normal samples here is larger than for those reported in Ref. 12. We suspect that this difference is due to the fact that the samples here and those in Ref. 12 were prepared in different sputter systems which yield multilayer films with different interfacial qualities. The Co layers in this study had 37% larger grain sizes (from x-ray diffraction measurements) and larger rms interfacial roughness (~3×, from atomic force microscopy measurements) than those in Ref. 12. A detailed understanding of the role of interfacial quality on ΔRA is still lacking, however.

Not surprisingly, we find that the ST switching is also susceptible to the reduced η_{eff} from the SAF. In Fig. 2(a) we show a ST scan for a SAF sample at low field (I ramp rate=0.5 mA/s) and a similar scan from a normal sample (1.0 mA/s) $Co_{fixed}(40)/Cu(10)/Co_{free}(3)/Cu(2)/Pt(30)$ (in nm), where the Co_{fixed} layer is unpatterned, in Fig. 2(b). We plot the current density J normalized to the Co_{free} layer thickness t because this is the value most directly related to the spin-torque.[12]

For four SAF samples, we measure $\Delta J_c/t=7\pm1\times10^7$ A/(cm^2 nm), while for 24 normal samples, $\Delta J_c/t=3.0\pm1.0\times10^7$ A/(cm^2 nm), an increase by a factor of ~2.3. Here, $\Delta J_c\equiv J_c^+-J_c^-$, where J_c^+ (J_c^-) is the critical current density for switching Co_{free} P to AP (AP to P) with Co_{fixed}. There is a small difference in the Cu spacer thickness between the SAF and normal devices, but this would only account for a 2% change in η_{eff}, which is well within our uncertainties. The polarization of the conduction electrons that exert a spin-torque on the Co_{free} layer may depend on the direction of the current flow. For J^-, electrons traverse the fixed layer (single Co or SAF) and are thereby spin filtered to produce a current with polarization η_- that impinges on the Co_{free} layer. For J^+, the incident electrons that are spin-filtered by the Co_{free} layer traverse the Cu spacer and impinge onto the fixed layer. From there a portion are reflected back to the Co_{free} layer, after being re-polarized η_+ by the spin-filtering effects of the fixed layer (single Co or SAF),

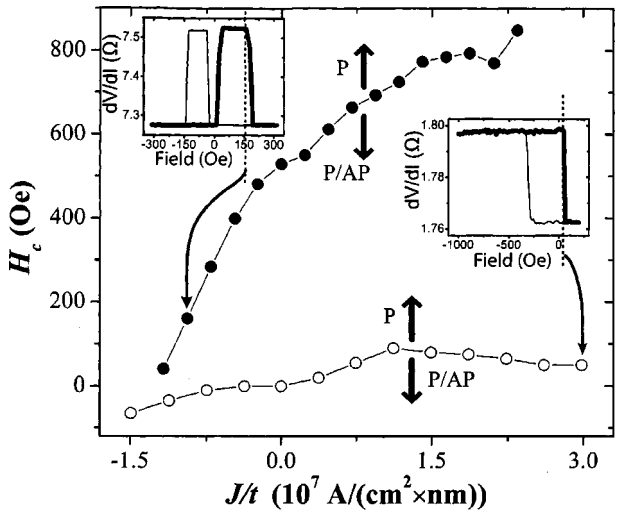

FIG. 3. H_c plotted vs J/t, the current density normalized to the Co_{free} layer thickness, for normal (●) and SAF (○) samples. The data illustrate the boundary separating the bistable P/AP region and the stable P region as shown. Insets show how H_c was measured.

and exert a spin-torque on the Co_{free} layer. For simplicity we assume that the effective polarization of the electron current exerting a spin-torque on the Co_{free} layer is the same in both cases, $\eta_{eff}=\eta_+=\eta_-$.

From Ref. 8, $\Delta J_c/t \propto \alpha[g(0,\eta)^{-1}+g(\pi,\eta)^{-1}]$. Here α is the Gilbert damping parameter and $g(\theta,\eta)$ is a measure of the spin-torque that is exerted on the free layer as a function of its alignment with the fixed layer and is a monotonically increasing function of η. Assuming $\eta_{eff}\approx 0.4$ and 0.2 for normal and SAF devices, respectively, and that α is the same for both types of devices, we plug these η_{eff} values into the $g(\theta,\eta)$ expression derived by Slonczewski[8] and find $[(\Delta J_c/t)_{SAF}]/[(\Delta J_c/t)_{normal}]\approx 2.5$, in reasonable agreement with the data.

We investigate the dependence of the ST $I-H$ phase diagram on η_{eff} by measuring the coercivity H_c of the Co_{free} layer as a function of J/t for both normal and SAF samples, shown in Fig. 3. The normal samples [same as those shown in Fig. 2(b)] have an unpatterned Co_{bottom} layer which has a naturally smaller H_c, making it simpler to identify the Co_{free} layer switching. These plots mark the respective boundaries between the bistable P/AP and P regions, as measured in other experiments with non-SAF samples.[3,18,19] The important point of Fig. 3 is that the slope of H_c versus J/t is much larger for normal samples than for SAF samples, highlighting the weaker influence, on the Co_{free} reversal, of the reduced η_{eff} in SAF samples. Spin-torque-induced excitations of a nanomagnet have been described by thermal activation models where either the effective barrier height or the temperature is modified by η_{eff} (Refs. 6, 20, and 21) and so a reduced η_{eff} correspondingly has a weaker influence on the activation process.

In summary, we have added Co_{bottom}/Ru layers to the familiar Co_{fixed}/Cu/Co_{free} CPP magnetic nanopillar composition. The Co_{bottom} and Co_{fixed} layers are AP due to exchange coupling through the Ru spacer and succeed in reducing unfavorable dipole fields on the Co_{free} layer. It is clear that these AP magnetic layers also reduce the spin polarization of I from the bulk Co value or single Co spin-filter value. Such reduction of the current polarization is advantageous for nanoscale devices seeking to reduce the effects of a spin-torque, such as CPP-GMR read heads,[9] where the reduction in ΔRA due to the SAF can be countered by partially oxidizing the magnetic interfaces.[22]

This work was supported by the NSF through the NSEC program. Fabrication was done at the Cornell Nanofabrication Facility which is a node of the NSF-supported National Nanofabrication Users Network.

[1] J. A. Katine, F. J. Albert, E. B. Myers, D. C. Ralph, and R. A. Buhrman, Phys. Rev. Lett. **84**, 3149 (2000).
[2] F. J. Albert, J. A. Katine, R. A. Buhrman, and D. C. Ralph, Appl. Phys. Lett. **77**, 3809 (2000).
[3] J. Grollier, V. Cros, A. Hamzic, J. M. George, H. Jaffrès, A. Fert, G. Faini, J. Ben Youssef, and H. Legall, Appl. Phys. Lett. **78**, 3663 (2000).
[4] J. E. Wegrowe, D. Kelly, Y. Jaccard, P. Guittienne, and J. P. Ansermet, Europhys. Lett. **45**, 626 (1999).
[5] J. Z. Sun, D. J. Monsma, D. W. Abraham, M. J. Rooks, and R. H. Koch, Appl. Phys. Lett. **81**, 2202 (2002).
[6] S. Urazhdin, N. O. Birge, W. P. Pratt, Jr., and J. Bass, Phys. Rev. Lett. **91**, 146803 (2003).
[7] L. Berger, Phys. Rev. B **54**, 9353 (1996).
[8] J. C. Slonczewski, J. Magn. Magn. Mater. **159**, L1 (1996).
[9] K. Nagasaka, Y. Seyama, R. Kondo, H. Oshima, Y. Shimizu, and A. Tanaka, Fujitsu Sci. Tech. J. **37**, 192 (2001).
[10] S. S. P. Parkin and D. Mauri, Phys. Rev. B **44**, 7131 (1991).
[11] S. S. P. Parkin, N. More, and K. P. Roche, Phys. Rev. Lett. **64**, 2304 (1990).
[12] F. J. Albert, N. C. Emley, E. B. Myers, D. C. Ralph, and R. A. Buhrman, Phys. Rev. Lett. **89**, 226802 (2002).
[13] L. Piraux, S. Dubois, A. Fert, and L. Belliard, Eur. Phys. J. B **4**, 413 (1998).
[14] K. Eid, R. Fonck, M. AlHaj Darwish, W. P. Pratt, Jr., and J. Bass, J. Appl. Phys. **91**, 8102 (2002).
[15] S. K. Upadhyay, R. N. Louie, and R. A. Buhrman, Appl. Phys. Lett. **74**, 3881 (1999).
[16] A. Rampe, D. Hartmann, W. Weber, S. Popovic, M. Reese, and G. Güntherodt, Phys. Rev. B **51**, 3230 (1995).
[17] L. Zhong and A. J. Freeman, J. Appl. Phys. **81**, 3890 (1997).
[18] E. B. Myers, F. J. Albert, J. C. Sankey, E. Bonet, R. A. Buhrman, and D. C. Ralph, Phys. Rev. Lett. **89**, 196801 (2002).
[19] S. I. Kiselev, J. C. Sankey, I. N. Krivorotov, N. C. Emley, R. J. Schoelkopf, R. A. Buhrman, and D. C. Ralph, Nature (London) **425**, 380 (2003).
[20] Z. Li and S. Zhang, cond-mat/0302339 (2003).
[21] R. H. Koch, J. A. Katine, and J. Z. Sun, Phys. Rev. Lett. **92**, 088302 (2004).
[22] K. Nagasaka, Y. Seyama, L. Varga, Y. Shimizu, and A. Tanaka, J. Appl. Phys. **89**, 6943 (2001).